

Optical and radio astrometry of the galaxy associated with FRB 150418

C. G. Bassa^{1*}, R. Beswick², S. J. Tingay^{3,4}, E. F. Keane^{5,6,7}, S. Bhandari^{6,7}, S. Johnston⁸, T. Totani⁹, N. Tominaga^{10,11}, N. Yasuda¹¹, B. W. Stappers², E. D. Barr⁶, M. Kramer^{12,2}, A. Possenti¹³

¹*ASTRON, the Netherlands Institute for Radio Astronomy, Postbus 2, NL-7990 AA Dwingeloo, The Netherlands*

²*Jodrell Bank Centre for Astrophysics, School of Physics and Astronomy, University of Manchester, Manchester M13 9PL, UK*

³*International Centre for Radio Astronomy Research (ICRAR), Curtin University, Bentley, WA 6102, Australia*

⁴*Istituto Nazionale di Astrofisica (INAF) – Istituto di Radio Astronomia, Via Piero Gobetti, Bologna, 40129, Italy*

⁵*Square Kilometre Array Organisation, Jodrell Bank Observatory, SK11 9DL, UK*

⁶*Centre for Astrophysics and Supercomputing, Swinburne University of Technology, Mail H29, PO Box 218, Victoria 3122, Australia*

⁷*Australian Research Council Centre of Excellence for All-sky Astrophysics (CAASTRO), Australia*

⁸*CSIRO Astronomy and Space Science, Australia Telescope National Facility, PO Box 76 Epping, NSW, 1710, Australia*

⁹*Department of Astronomy, the University of Tokyo, Hongo, Tokyo 113-0033, Japan*

¹⁰*Department of Physics, Faculty of Science and Engineering, Konan University, 8-9-1 Okamoto, Kobe, Hyogo 658-8501, Japan*

¹¹*Kavli Institute for the Physics and Mathematics of the Universe (WPI), Institutes for Advanced Study, University of Tokyo, Kashiwa, Chiba 277-8583, Japan*

¹²*Max-Planck-Institut für Radioastronomie (MPIfR), Auf dem Hügel 69, D-53121 Bonn, Germany*

¹³*Istituto Nazionale di Astrofisica (INAF)-Osservatorio Astronomico di Cagliari, Via della Scienza 5, I-09047 Selargius (CA), Italy*

Accepted 27 July 2016. Received 2016 July 5; in original form 2016 May 12

ABSTRACT

A fading radio source, coincident in time and position with the fast radio burst FRB 150418, has been associated with the galaxy WISE J071634.59–190039.2. Subsequent observations of this galaxy have revealed that it contains a persistent, but variable, radio source. We present e-MERLIN, VLBA, and ATCA radio observations and Subaru optical observations of WISE J071634.59–190039.2 and find that the persistent radio source is unresolved and must be compact (< 0.01 kpc), and that its location is consistent with the optical centre of the galaxy. We conclude that it is likely that WISE J071634.59–190039.2 contains a weak radio AGN.

Key words: stars: neutron, magnetars – pulsars: general – galaxies: active

1 INTRODUCTION

Fast radio bursts (FRBs, see e.g. Petroff et al. 2016 and references therein) are millisecond-duration bursts of radio emission that have been observed at the Parkes, Arecibo, and Green Bank radio telescopes (Lorimer et al. 2007; Spitler et al. 2014; Masui et al. 2015). FRBs have dispersion measures (DMs), a measure of the electron column density, that range from 1.4 to 33 times the maximum Galactic contribution (Cordes & Lazio 2002), thought to be attributable to free electrons in the intergalactic medium. With this interpretation the distances to FRBs are cosmological (Lorimer et al. 2007; Thornton et al. 2013), and the corresponding luminosities of the FRB signals are thus many orders of magnitude higher than typical pulsar luminosities.

Non-cosmological explanations have been put forward (e.g. Burke-Spolaor et al. 2011; Loeb et al. 2014; Kulkarni et al. 2014) but a cosmological interpretation remains favored, based on current observational evidence. While the extragalactic interpretation of FRBs currently prevails, their progenitor(s) are as yet unknown. In an effort to determine the nature of FRBs, the SURvey for Pulsars and Extragalactic Transients (SUPERB) performs real time FRB searches at the Parkes telescope, and employs an array of multi-wavelength telescopes to follow up FRB discoveries. Multi-wavelength follow-up of FRB 150418 led, for the first time, to the detection of a fading radio source that was associated with a galaxy at $z = 0.49$ (Keane et al. 2016). This galaxy is also detected in the mid-infrared by WISE (Wright et al. 2010) and cataloged as WISE J071634.59–190039.2.

Radio imaging observations of WISE J071634.59–190039.2 with the Australia Telescope Compact Array (ATCA) showed a

* email: bassa@astron.nl

source declining by a factor ~ 3 in brightness at 5.5 GHz during the first 6 d after the FRB. This source subsequently settled at a persistent brightness of approximately $100 \mu\text{Jy beam}^{-1}$. Comparing this behaviour to the results of transient surveys (Bell et al. 2015; Moolley et al. 2016) led Keane et al. (2016) to argue in favour of the association between FRB 150418 and the fading radio source, and hence with the galaxy.

The association of FRB 150418 with the fading radio source and hence with WISE J071634.59–190039.2 met with criticism. JVLA observations of the persistent radio source in WISE J071634.59–190039.2 showed rapid variability, which led Williams & Berger (2016) to argue that the variability of the fading radio source is consistent with the intrinsic or scintillating behaviour of a compact, weak active galactic nucleus (AGN). Similarly, Akiyama & Johnson (2016) show that the variability of the persistent source may be extrinsic and attributable to refractive scintillation in the Milky Way, assuming a compact radio source is present in the galaxy. Vedantham et al. (2016) find a flat radio spectrum for the persistent source and suggest it is consistent with the properties of an AGN.

Since FRB 150418 is the first FRB for which a radio counterpart and host galaxy have been suggested, the host galaxy warrants closer study. In this Letter we report on an astrometric radio and optical analysis that establishes that WISE J071634.59–190039.2 currently contains a single weak, compact radio source consistent with an AGN located at the centre of the galaxy.

2 OBSERVATIONS AND ANALYSIS

2.1 ATCA

We observed WISE J071634.59–190039.2 with the ATCA on 2016 March 1 at 05:30 UTC for a duration of 11 hours. Observations were made in 6B configuration, in two frequency bands each with bandwidth 2 GHz centered at 5.5 and 7.5 GHz respectively. Single pointing mode was used which yielded an image rms of $6 \mu\text{Jy beam}^{-1}$ with an angular resolution of $1''.9 \times 10''.4$. Bandpass and flux density calibration were carried out using the standard ATCA calibrators B1934–638 and B0823–500 and phase calibration with B0733–174. Data reduction was performed in MIRIAD (Sault et al. 1995) using standard techniques and the position of sources in the field were measured using the task IMFIT. The position is listed in Table 1. In addition, we used the mosaic observations made with the ATCA on 2015 October 27 and described in Keane et al. (2016) to measure the positions of four other sources in the field (Table 2).

2.2 e-MERLIN

WISE J071634.59–190039.2 was observed with the e-MERLIN array on 2016 March 18, 21 and 22 between 17:00 and 21:50 UTC on each day at C-band (4.816–5.328 GHz). The e-MERLIN array comprised of six telescopes for each of these observations. The 76-m Lovell telescope was not included. Data were correlated in full Stokes mode in a standard C-band configuration with 4×128 MHz bands. The target and phase calibrator (J0718–1813) were observed with a 7:3 minute phase referencing cycle. In addition, every hour, one target scan was re-deployed to observe a faint nearby NVSS radio source (J0716–1908) in order to verify calibration. Observations of 3C286 and OQ208 (30 mins each) were made for flux density and bandpass calibration.

Each observing run was reduced independently and in an identical manner. Data were imported into AIPS (Greisen 2003) using the e-MERLIN pipeline (Argo 2015). Following editing, these data were fringe-fitted for delay only and flux density calibrated using 3C286 relative to the Perley & Butler (2013) flux density scale. Bandpass solutions were derived using the point source calibrator OQ208. Standard phase referencing calibration was applied using the nearby phase calibrator source J0718–1813. These phase and amplitude calibration solutions were then applied to both the target and check calibration source (J0716–1908) which were subsequently imaged using standard techniques.

Following initial imaging of individual epochs, data from all three observing runs were concatenated together to increase sensitivity. These data were then re-weighted in a time and frequency dependent manner to maximize the sensitivity. An unresolved radio source associated with WISE J071634.59–190039.2 was detected with a measured peak brightness of $151 \mu\text{Jy beam}^{-1}$ and an image rms of $21 \mu\text{Jy beam}^{-1}$. The angular resolution is $0''.251 \times 0''.030$ at a position angle of $11^\circ.8$. In addition to the target source, two in-beam radio sources were detected. The coordinates of these sources and WISE J071634.59–190039.2 are listed in Tables 1 and 2.

In addition to these C-band observations, e-MERLIN also observed at L-band (1.25–1.75 GHz) on 2016 Apr 2 between 16:15 and 21:00 UTC. These observations utilized all e-MERLIN telescopes including the Lovell telescope. Data were correlated across 512 MHz of bandwidth and divided into 8 bands. The same phase calibration source (J0718–1813) as employed at C-band was used, and data were reduced in an identical manner.

Following wide field imaging of the target field at L-band, e-MERLIN detected 7 radio sources within the wider field of view accessible to the array. The positions of these sources are listed in Table 2. Radio emission at the location of the target source, WISE J071634.59–190039.2, was detected at a peak flux density of $92 \pm 19 \mu\text{Jy beam}^{-1}$. The angular resolution is $0''.46 \times 0''.32$ at a position angle of $-6^\circ.6$.

2.3 VLBA

The Very Long Baseline Array (VLBA; Napier et al. 1994) was used to observe WISE J071634.59–190039.2 on 2016 March 8, 00:30–06:30 UTC at C-band (4.852–5.108 GHz). Data were recorded in dual circular polarization mode for 8×32 MHz bands with 2-bit Nyquist sampling, corresponding to an aggregate recorded data rate of 2048 Mbps. All ten antennas of the VLBA were used. As well as the target galaxy, two phase reference sources were observed, J0719–1955 and J0718–1813 (same phase calibrator as used for e-MERLIN). Observations of each individual phase reference source were made once per 10 minutes, but interleaved such that a calibrator was observed every 5 minutes.

The data were correlated using the DiFX software correlator (Deller et al. 2007, 2011) using an integration time of 1.024 seconds and with 64 frequency channels per 32 MHz of bandwidth. As well as correlation phase centers set on the target galaxy and phase reference positions, additional phase centers (J2000) were correlated, for sources known from our ATCA imaging within the VLBA primary beam while pointed at the target galaxy. Four additional phase centers were correlated ($\alpha_{J2000}, \delta_{J2000}$): ($07^{\text{h}}16^{\text{m}}39^{\text{s}}.41, -18^{\circ}56'29''.2$); ($07^{\text{h}}16^{\text{m}}04^{\text{s}}.04, -19^{\circ}00'14''.7$); ($07^{\text{h}}16^{\text{m}}05^{\text{s}}.47, -19^{\circ}00'15''.9$); and ($07^{\text{h}}16^{\text{m}}14^{\text{s}}.41, -19^{\circ}06'49''.9$).

The correlated data were processed in AIPS (Greisen 2003) using standard phase reference techniques. System temperature and

Table 1. Radio and optical positions for WISE J071634.59–190039.2. The uncertainties of the Subaru positions have the uncertainty in the astrometric calibration added in quadrature.

Telescope	Band	α_{J2000}	δ_{J2000}
e-MERLIN	L	07 ^h 16 ^m 34 ^s .554(2)	−19°00′39″.42(5)
e-MERLIN	C	07 ^h 16 ^m 34 ^s .5550(4)	−19°00′39″.466(18)
VLBA	C	07 ^h 16 ^m 34 ^s .5550(1)	−19°00′39″.476(3)
ATCA	C	07 ^h 16 ^m 34 ^s .573(10)	−19°00′38″.6(7)
Subaru	<i>i'</i>	07 ^h 16 ^m 34 ^s .556(7)	−19°00′39″.53(8)

gain information for each antenna was used to calibrate the visibility amplitudes, in addition to corrections for sampler thresholds. Corrections for instrumental effects, Earth orientation parameters, and ionosphere were applied to the visibility phases. The data for the two phase reference calibrators were then fringe-fitted, exported from AIPS, and imaged in DIFMAP (Shepherd et al. 1995). The images were imported to AIPS and used as source brightness models in a second round of fringe-fitting, to account for their structure contributions to the visibility phases. The resultant phase corrections were smoothed over a 0.4-hour period using boxcar averaging. The final aggregate amplitude and phase corrections were transferred to the correlated data for each of the target and in-beam radio sources and applied to the visibilities before writing the data to disk as FITS files, retaining full frequency channelization.

The FITS files were read in to MIRIAD and naturally weighted Stokes I images ($\pm 1''$ 5 around the phase centre position) were produced, using multi-frequency synthesis to avoid bandwidth smearing, with 0.3 mas pix^{-1} sizes (10,000 pixel images). The target radio source associated with WISE J071634.59–190039.2 was detected with a peak brightness of $130 \mu\text{Jy beam}^{-1}$ and an image rms of $14 \mu\text{Jy beam}^{-1}$. The position, obtained using task MAXFIT and checked with task IMFIT, is listed in Table 1. The uncertainty on the position includes the uncertainty on the position of the phase reference calibrators ($\approx 1 \text{ mas}$ in both coordinates) as given by Petrov et al. (2006). No evidence of resolved emission is seen and the object appears point-like ($< 1.5 \text{ mas}$ in extent). The angular resolution (full width at half maximum of the point spread function) of the VLBA images is $0.9 \text{ mas} \times 2.6 \text{ mas}$ at a position angle of -3.4 . Two of the in-beam sources were also detected, and coincide with e-MERLIN and ATCA sources 1 and 2 (see Table 2).

2.4 Subaru

Optical observations of the field containing FRB 150418 were obtained with Suprime-Cam on the 8.2-m Subaru telescope. Here, we use the *i'*-band observation obtained on 2015, April 19 with a dithered set of $10 \times 60 \text{ s}$ exposures. Suprime-Cam is a mosaic of ten $4\text{k} \times 2\text{k}$ detectors, covering a field-of-view of $34' \times 27'$ sampled at $0''.2 \text{ pix}^{-1}$. The individual images were reduced using the Hyper-Suprime-Cam pipeline version 3.8.5, which is developed based on the LSST pipeline (Ivezic et al. 2008; Axelrod et al. 2010). Following the bias subtraction and flatfielding, the astrometry of all images is simultaneously solved with a 5th order polynomial to represent the optical distortion. Here we used 4606 stars for the fitting to the external catalog and 3826 stars for the internal fitting. The weights of images for co-adding them are also derived according to their signal-to-noise ratios. Thereafter, the individual images were mapped to pixels on a world coordinate system and a

Table 2. Radio and optical positions 7 sources in the field-of-view. The uncertainties of the Subaru positions have the uncertainty in the astrometric calibration added in quadrature.

Telescope	Band	α_{J2000}	δ_{J2000}
Source 1 (NVSS J071639–185620)			
e-MERLIN	L	07 ^h 16 ^m 39 ^s .408(2)	−18°56′29″.93(3)
e-MERLIN	C	07 ^h 16 ^m 39 ^s .4080(5)	−18°56′29″.89(2)
VLBA	C	07 ^h 16 ^m 39 ^s .4082(1)	−18°56′29″.890(3)
ATCA	C	07 ^h 16 ^m 39 ^s .410(2)	−18°56′29″.30(19)
Subaru	<i>i'</i>	07 ^h 16 ^m 39 ^s .408(7)	−18°56′30″.06(9)
Source 2 (NVSS J071604–190015)			
e-MERLIN	L	07 ^h 16 ^m 04 ^s .037(2)	−19°00′15″.78(3)
e-MERLIN	C	07 ^h 16 ^m 04 ^s .0370(6)	−19°00′15″.86(3)
VLBA	C	07 ^h 16 ^m 04 ^s .0355(1)	−19°00′15″.775(3)
ATCA	C	07 ^h 16 ^m 04 ^s .034(1)	−19°00′14″.79(15)
Subaru	<i>i'</i>	07 ^h 16 ^m 04 ^s .030(7)	−19°00′15″.83(8)
Source 3			
e-MERLIN	L	07 ^h 16 ^m 05 ^s .475(2)	−19°00′16″.88(3)
ATCA	C	07 ^h 16 ^m 05 ^s .470(4)	−19°00′15″.9(4)
Subaru	<i>i'</i>	07 ^h 16 ^m 05 ^s .467(8)	−19°00′16″.78(10)
Source 4			
e-MERLIN	L	07 ^h 16 ^m 14 ^s .405(2)	−19°06′50″.47(4)
ATCA	C	07 ^h 16 ^m 14 ^s .403(7)	−19°06′49″.8(7)
Source 5			
e-MERLIN	L	07 ^h 16 ^m 02 ^s .558(3)	−19°08′19″.89(4)
Source 6			
e-MERLIN	L	07 ^h 16 ^m 19 ^s .356(3)	−19°13′56″.94(4)
Source 7			
e-MERLIN	L	07 ^h 16 ^m 47 ^s .200(3)	−18°45′25″.26(5)

weighted mean of each pixel value was computed with clipping of 3σ outliers.

To calibrate the astrometry of this co-added image, we compared the centroids of stars on a $14' \times 14'$ subsection with several astrometric catalogs. We selected only bright ($K < 14$) stars from the 2MASS catalog (Cutri et al. 2003; Skrutskie et al. 2006) that matched objects on the Suprime-Cam image that were not saturated and appeared stellar and unblended. Iteratively rejecting outliers with residuals in excess of $0''.25$, the final astrometric calibration, fitting for zero-point position, and a four parameter transformation matrix, uses 88 stars and yields rms residuals of $0''.058$ in right ascension and $0''.060$ in declination.

Since the 2MASS catalog does not provide proper motions, the calibration might have a systematic positional offset due to non-random proper motions over the $\sim 15 \text{ yr}$ time baseline between the 2MASS observations and the Subaru observation. To investigate the effect of proper motion we also calibrated the same subsection of the Suprime-Cam image against the 4th version of the USNO CCD Astrograph Catalog (UCAC4; Zacharias et al. 2013). This catalog provides proper motions by combining positional CCD measurements obtained between 1998 and 2004 with positions from historic astrograph plates. Propagating the UCAC4 positions to the epoch of the Subaru observations, and applying the same procedure as with 2MASS, we obtain an astrometric calibration using 78

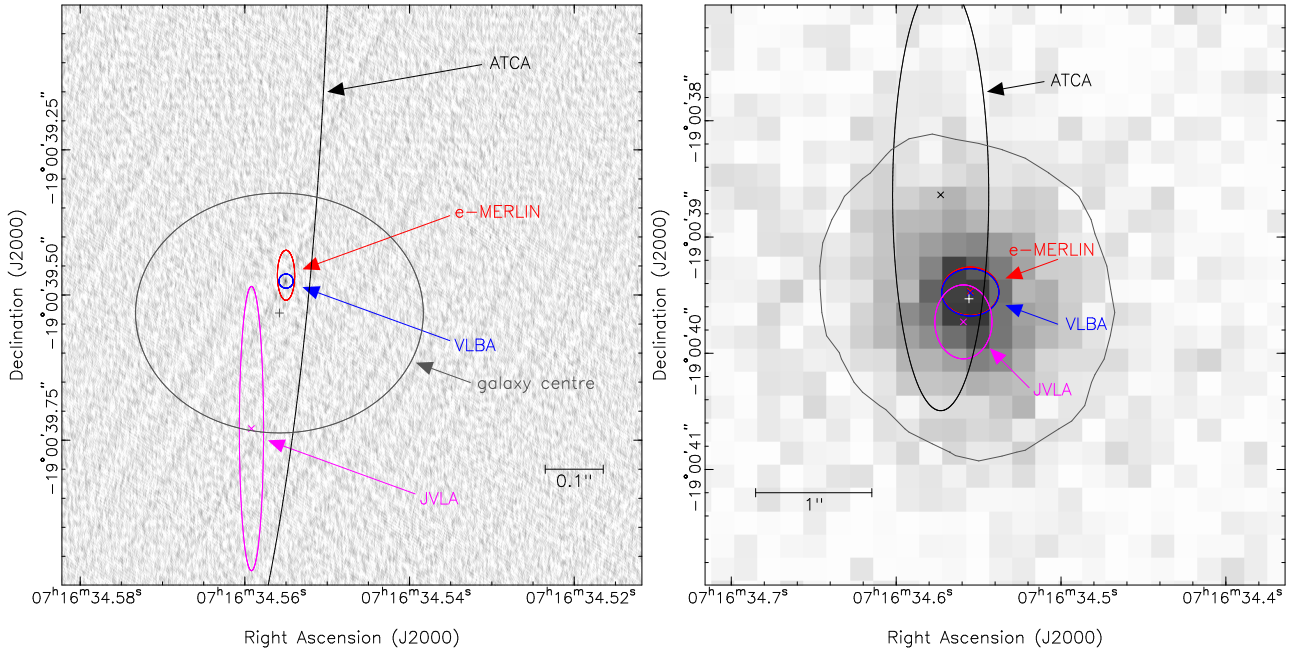


Figure 1. The right panel shows a $1'' \times 1''$ subsection of the VLBA radio image of the galaxy centre. Here, the position and uncertainty of the optical centre of the galaxy are shown with the plus sign and the ellipse (95% confidence). The left panel shows a $5'' \times 5''$ subsection of the 600 s Subaru Supreme-Cam i' -band image of the WISE J071634.59–190039.2 galaxy. The centre of light of the galaxy on the image is marked by the white plus sign. The dark grey contour traces the half-light radius as defined by Keane et al. (2016). In both panels, the 95% confidence uncertainties on the positions of the radio source seen by e-MERLIN, VLBA, ATCA and JVLA (Vedantham et al. 2016) are shown with the ellipses. Note that in the right panel, these include the uncertainty in the astrometric calibration of the Subaru image, hence the differences in error region sizes between the two panels.

stars and rms residuals of $0''.101$ in right ascension and $0''.083$ in declination.

Based on the UCAC4 calibration, the centre of light of WISE J071634.59–190039.2 is offset from the position based on the 2MASS calibration by $0''.047$ in right ascension and $0''.025$ in declination. Since the UCAC4 calibration corrects for proper motion and encloses the positional uncertainty of WISE J071634.59–190039.2 based on the 2MASS calibration, we use the UCAC4 calibration for the remainder of the paper. Of the 7 additional radio sources detected by e-MERLIN at L-band, 6 overlap with the full Subaru image, and 3 have optical counterparts above the 5σ limit of $i' = 24.7$. The positions of these counterparts, as well as that of WISE J071634.59–190039.2 are given in Table 1 and 2. The optical positions of these counterparts are consistent with the radio positions, providing independent confirmation that the astrometric calibration is correct.

3 DISCUSSION

A single unresolved radio source is detected in the ATCA, e-MERLIN and VLBA observations of WISE J071634.59–190039.2. The source has a brightness of 130 to 151 $\mu\text{Jy beam}^{-1}$ at frequencies between approximately 4.8 and 5.3 GHz, consistent within the uncertainties. The coordinates derived from the ATCA, e-MERLIN and VLBA observations are in agreement and are consistent with previously reported ATCA (Keane et al. 2016) coordinates. These detections are consistent with the low significance detection at the same position with the EVN, reported by Marcote et al. (2016a,b), after our high resolution astrometry was first reported as an ATel (Bassa et al. 2016). We note that the JVLA position by Vedantham

et al. (2016) is inconsistent in right ascension with our e-MERLIN and VLBA positions.

The coordinates of the compact radio source are plotted in Figure 1 and are overlaid on the Subaru Supreme-Cam i' -band image of WISE J071634.59–190039.2 that was obtained on 2015, April 19, as well as the VLBA radio image. We conservatively plot 95% confidence uncertainty regions of the radio source positions. The optical centre of light of WISE J071634.59–190039.2 is offset from the C-band VLBA and e-MERLIN positions by $\Delta\alpha = 0''.01(10)$ and $\Delta\delta = -0''.05(8)$. On this basis, our astrometry shows that, within the uncertainties quoted above, the location of the compact radio source is consistent with the optical centre of light of WISE J071634.59–190039.2 in the Subaru i' -band image.

The compact radio source detected recovers a very high percentage of the persistent flux density reported by Keane et al. (2016) and Vedantham et al. (2016), indicating that little, if any, extended radio emission exists. The upper limit to the size of the radio source of < 1.5 mas (implying a brightness temperature in excess of 5×10^6 K), corresponds to a physical size of less than 0.01 kpc at a redshift of $z = 0.49$. An interpretation of the radio emission as due to a star formation region therefore appears highly unlikely as circumnuclear star formation regions (e.g. NGC 253; Lenc & Tingay 2006), those associated with merger activity (Engel et al. 2011), or jet induced star formation regions (Salomé et al. 2015), are generally two orders of magnitude larger than our upper limit. Furthermore, the observed brightness temperature exceeds that expected from thermal radio emission processes associated with star formation regions. The location of the compact radio source is consistent with our best estimate of the centre of its host galaxy. Thus, our data are consistent with the existence of a weak radio AGN within the galaxy (see Guidetti et al. 2013 for a discussion of the existence of AGN in ‘radio quiet’ galaxies).

While the emission of the persistent source can be shown to be compact on VLBI angular scales (milliarcseconds), interstellar scintillation requires structure which is compact on far smaller scales (microarcseconds; Macquart et al. 2013). Our ATCA, e-MERLIN and VLBA observations cannot directly probe the required angular scales. Hence, the presence of a compact persistent radio source such as an AGN in WISEJ071634.59–190039.2 allows the scenario proposed by Williams & Berger (2016) and Akiyama & Johnson (2016); that the fading radio source coincident in position with WISEJ071634.59–190039.2 and coincident in time with FRB 150418 could be due to interstellar scintillation.

The best probe of the scintillation interpretation will come from extensive radio photometry measurements, as the signature of scintillation is well known and can be tested against the data (Akiyama & Johnson 2016). A careful analysis of all available flux density measurements of WISEJ071634.59–190039.2 from the ATCA, JVLA, e-MERLIN, VLBA, EVN, and other facilities should reveal whether the variability properties of the compact radio source are consistent with intrinsic AGN variability or scintillation.

ACKNOWLEDGMENTS

We thank both e-MERLIN and NRAO for providing observations under Director’s Discretionary Time, and Sarah Burke Spolaor for helping with the VLBA observations. This paper makes use of software developed for the Large Synoptic Survey Telescope. We thank the LSST Project for making their code available as free software at <http://dm.lsstcorp.org>. The National Radio Astronomy Observatory is a facility of the National Science Foundation operated under cooperative agreement by Associated Universities, Inc. The Australian Telescope Compact Array is part of the Australia Telescope National Facility which is funded by the Commonwealth of Australia for operation as a National Facility managed by CSIRO. This work was based in part on data collected at Subaru Telescope, which is operated by the National Astronomical Observatory of Japan. CGB acknowledges support from the European Research Council under the European Union’s Seventh Framework Programme (FP/2007-2013) / ERC Grant Agreement nr. 337062 (DRAGNET; PI Hessels). SJT is a Western Australian Premier’s Research Fellow. TT was supported by JSPS KAKENHI Grant Numbers 15K05018 and 40197778. NT is supported by the Toyota Foundation (D11-R-0830). EK and SB acknowledge the support of the Australian Research Council Centre of Excellence for All-sky Astrophysics (CAASTRO), through project number CE110001020. This research has made use of NASA’s Astrophysics Data System.

REFERENCES

Akiyama K., Johnson M. D., 2016, *ApJ*, 824, L3
 Argo M., 2015, preprint, ([arXiv:1502.04936](https://arxiv.org/abs/1502.04936))
 Axelrod T., Kantor J., Lupton R. H., Pierfederici F., 2010, in *Software and Cyberinfrastructure for Astronomy*. p. 774015, [doi:10.1117/12.857297](https://doi.org/10.1117/12.857297)
 Bassa C., et al., 2016, *The Astronomer’s Telegram*, 8938
 Bell M. E., Huynh M. T., Hancock P., Murphy T., Gaensler B. M., Burlon D., Trott C., Bannister K., 2015, *MNRAS*, 450, 4221
 Burke-Spolaor S., Bailes M., Ekers R., Macquart J.-P., Crawford III F., 2011, *ApJ*, 727, 18
 Cordes J. M., Lazio T. J. W., 2002, preprint, ([arXiv:0207156](https://arxiv.org/abs/0207156))
 Cutri R. M., et al., 2003, *VizieR Online Data Catalog*, 2246

Deller A. T., Tingay S. J., Bailes M., West C., 2007, *PASP*, 119, 318
 Deller A. T., et al., 2011, *PASP*, 123, 275
 Engel H., Davies R. I., Genzel R., Tacconi L. J., Sturm E., Downes D., 2011, *ApJ*, 729, 58
 Greisen E. W., 2003, *Information Handling in Astronomy - Historical Vistas*, 285, 109
 Guidetti D., Bondi M., Prandoni I., Beswick R. J., Muxlow T. W. B., Wrigley N., Smail I., McHardy I., 2013, *MNRAS*, 432, 2798
 Ivezić Z., et al., 2008, preprint, ([arXiv:0805.2366](https://arxiv.org/abs/0805.2366))
 Keane E. F., et al., 2016, *Nature*, 530, 453
 Kulkarni S. R., Ofek E. O., Neill J. D., Zheng Z., Juric M., 2014, *ApJ*, 797, 70
 Lenc E., Tingay S. J., 2006, *AJ*, 132, 1333
 Loeb A., Shvartzvald Y., Maoz D., 2014, *MNRAS*, 439, L46
 Lorimer D. R., Bailes M., McLaughlin M. A., Narkevic D. J., Crawford F., 2007, *Science*, 318, 777
 Macquart J.-P., Godfrey L. E. H., Bignall H. E., Hodgson J. A., 2013, *ApJ*, 765, 142
 Marcote B., Giroletti M., Garrett M., Yang J., Paragi Z., Hada K., Cheung C. C., 2016a, *The Astronomer’s Telegram*, 8865
 Marcote B., Giroletti M., Garrett M., Yang J., Paragi Z., Hada K., Cheung C. C., 2016b, *The Astronomer’s Telegram*, 8959
 Masui K., et al., 2015, *Nature*, 528, 523
 Mooley K. P., et al., 2016, *ApJ*, 818, 105
 Napier P. J., Bagri D. S., Clark B. G., Rogers A. E. E., Romney J. D., Thompson A. R., Walker R. C., 1994, *IEEE Proceedings*, 82, 658
 Perley R. A., Butler B. J., 2013, *ApJS*, 204, 19
 Petroff E., et al., 2016, preprint, ([arXiv:1601.03547](https://arxiv.org/abs/1601.03547))
 Petrov L., Kovalev Y. Y., Fomalont E. B., Gordon D., 2006, *AJ*, 131, 1872
 Salomé Q., Salomé P., Combes F., 2015, *A&A*, 574, A34
 Sault R. J., Teuben P. J., Wright M. C. H., 1995, in Shaw R. A., Payne H. E., Hayes J. J. E., eds, *Astronomical Society of the Pacific Conference Series Vol. 77, Astronomical Data Analysis Software and Systems IV*. p. 433 ([arXiv:astro-ph/0612759](https://arxiv.org/abs/astro-ph/0612759))
 Shepherd M. C., Pearson T. J., Taylor G. B., 1995, in Butler B. J., Muhleman D. O., eds, *BAAS Vol. 27, Bulletin of the American Astronomical Society*. p. 903
 Skrutskie M. F., et al., 2006, *AJ*, 131, 1163
 Spitler L. G., et al., 2014, *ApJ*, 790, 101
 Thornton D., et al., 2013, *Science*, 341, 53
 Vedantham H. K., Ravi V., Mooley K., Frail D., Hallinan G., Kulkarni S. R., 2016, *ApJ*, 824, L9
 Williams P. K. G., Berger E., 2016, *ApJ*, 821, L22
 Wright E. L., et al., 2010, *AJ*, 140, 1868
 Zacharias N., Finch C. T., Girard T. M., Henden A., Bartlett J. L., Monet D. G., Zacharias M. I., 2013, *AJ*, 145, 44

This paper has been typeset from a $\text{\TeX}/\text{\LaTeX}$ file prepared by the author.